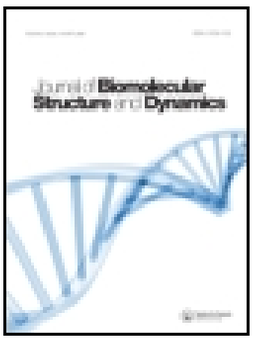

Journal of Biomolecular Structure and Dynamics

ISSN: 0739-1102 (Print) 1538-0254 (Online) Journal homepage: http://www.tandfonline.com/loi/tbsd20

Structural investigations into the binding mode of a novel noscapine analogue, 9-(4-vinylphenyl) noscapine, with tubulin by biochemical analyses and molecular dynamic simulations

Tejashree Mahaddalkar, Pradeep Kumar Naik, Sinjan Choudhary, Naresh Manchukonda, Srinivas Kantevari & Manu Lopus

To cite this article: Tejashree Mahaddalkar, Pradeep Kumar Naik, Sinjan Choudhary, Naresh Manchukonda, Srinivas Kantevari & Manu Lopus (2016): Structural investigations into the binding mode of a novel noscapine analogue, 9-(4-vinylphenyl) noscapine, with tubulin by biochemical analyses and molecular dynamic simulations, Journal of Biomolecular Structure and Dynamics, DOI: 10.1080/07391102.2016.1222969

To link to this article: http://dx.doi.org/10.1080/07391102.2016.1222969

Journal of Biomolecular Structure and Dynamics, 2016
http://dx.doi.org/10.1080/07391102.2016.1222969

Taylor & Francis
Taylor & Francis Group

LETTER TO THE EDITOR

Structural investigations into the binding mode of a novel noscapine analogue, 9-(4-vinylphenyl) noscapine, with tubulin by biochemical analyses and molecular dynamic simulations

Tejashree Mahaddalkar[a], Pradeep Kumar Naik[b,1], Sinjan Choudhary[a], Naresh Manchukonda[c], Srinivas Kantevari[c] and Manu Lopus[a]*

[a]*Experimental Cancer Therapeutics and Chemical Biology, UM-DAE Centre for Excellence in Basic Sciences, University of Mumbai Kalina Campus, Santacruz (E), Mumbai 400098, India;* [b]*Department of Biotechnology, Guru Ghasidas Central University, Bilaspur, Chattisgarh 495009, India;* [c]*Organic Chemistry Division-II (CPC Division), CSIR-Indian Institute of Chemical Technology, Hyderabad, Telangana 500007, India*

Communicated by Ramaswamy H. Sarma

(*Received 13 May 2016; accepted 4 August 2016*)

Keywords: microtubules; molecular dynamic simulations; tubulin isotypes; β_{III} tubulin; noscapine; 9-(4-vinylphenyl) noscapine

Introduction

Tubulin, the basic building block of microtubules, is composed of one α and one β subunit. The β tubulin has eight well-characterized *isotypes* that show slight variations at their C-terminal amino acid composition (Janke, 2014). Although multiple factors would work in tandem to induce drug resistance in cancer chemotherapy with combinatorial regimens, one major challenge in tubulin-targeted therapeutics is resistance associated with overexpression of the β_{III} isotype (Lopus et al., 2015; Stengel et al., 2010)

The antitussive plant alkaloid noscapine and its congeners have been known for their antitumour efficacy and safe pharmacological profiles (Lopus & Naik, 2015). Recently, we synthesized a potent derivative of noscapine, 9-(4-vinylphenyl) noscapine (VinPhe-Nos) that inhibited proliferation of human cancer cell lines, such as cervical carcinoma (HeLa; IC_{50}, 20.3 μM), lung carcinoma (A549; IC_{50}, 42.7 μM), and breast carcinoma (MCF-7; IC_{50}, 34.3 μM), at low micro-molar range (Santoshi et al., 2015). In this study, we report the fine details of the molecular-level interactions of VinPhe-Nos with tubulin. After ensuring that the drug is several times more potent than noscapine in inhibiting cancer cell proliferation, we characterized the binding interactions of VinPhe-Nos with purified tubulin using a combination of biophysical and biochemical analyses. Finally, using a combination of molecular docking, molecular dynamic (MD) simulation, and predictive binding energy calculation based on Prime/molecular mechanics-generalized Born/surface area (Prime/MM-GBSA) continuum solvent model, we elucidated the mode of interactions of VinPhe-Nos with all known isotypes of tubulin.

Materials and methods

VinPhe-Nos was synthesized from noscapine using optimized Suzuki reaction conditions as described earlier (Santoshi et al., 2015). 8-anilino-1-naphthalenesulfonic acid (ANS), guanosine-5′-triphosphate (GTP), piperazine-N,N′-bis(2-ethanesulfonic acid) (Pipes), magnesium sulfate ($MgSO_4$), and ethylene glycol tetraacetic acid (EGTA), were purchased from Sigma (St. Louis, MO). All other reagents were of analytical grade.

Spectral measurements

Fluorescence spectra were measured using a FlouroMax® 4 spectrofluorometer (Horiba Scientific, Edison, NJ) supported by FluorEssence 3.5 software. Far-UV circular dichroism spectra were obtained using JASCO-810 CD spectrophotometer (JASCO, Tokyo, Japan). A .2-cm path-length quartz cuvette was used for reading the samples. Absorbance measurements were carried out using a Shimadzu UV-1800 spectrophotometer (Shimadzu, Kyoto, Japan).

Cell culture

MDA-MB-231 cells were obtained from American Type Culture Collection (ATCC), and were cultured in

*Corresponding author. Email: manu.lopus@cbs.ac.in
[1]Present address: School of Life Sciences, Sambalpur University, Jyoti Vihar, Sambalpur, Odisha 768019, India

Dulbecco's Modified Eagle Medium (DMEM; Invitrogen, Carlsbad, CA), supplemented with 10% fetal bovine serum (FBS; Invitrogen), 50 μg/ml penicillin and streptomycin, and 2 mM glutamine (Life Technologies, Carlsbad, CA). The cells were maintained in a Forma Stericycle incubator (Thermo Scientific, Waltham, MA) at 37°C and 5% CO_2. After every two months of use, the culture was discarded and a new stock revived. The cells were determined to be free of mycoplasma as indicated by Hoechst 33342 staining (Life Technologies) and MycoAlert Mycoplasma detection kit (Lonza, Basel, Switzerland).

Cell viability assay

The cell viability assay was performed in 12-well plates. MDA-MB-231 cells were seeded at a density of 7.5×10^4 cells/mL. The next day, they were treated with different concentrations of VinPhe-Nos (0–100 μM) for 72 h at 37°C. Subsequently, the media aspirated off, and the cells were detached by trypsinization. The number of viable cells in each well was determined by manual counting of the trypan blue (Amresco, Solon, OH)-stained cells. The experiment was repeated twice.

Tubulin purification

Microtubule-associated proteins-free (MAPs-free) tubulin was purified from goat brain through cycles of temperature- and GTP-dependent assembly and disassembly, as described previously (Mahaddalkar, Suri, Naik, & Lopus, 2015). The protein concentration was determined by the method of Bradford, using bovine serum albumin (BSA) as the standard (Mahaddalkar et al., 2015), and the protein has been stored at −80°C until used.

Circular dichroism

To probe the conformational change in the tubulin secondary structures when bound to VinPhe-Nos, circular dichroism measurements were used. The CD spectrophotometer was thoroughly purged with nitrogen before starting the experiments. Tubulin (5 μM) was incubated with 50 μM VinPhe-Nos in 25 mM Pipes buffer, pH 6.8, for 30 min at 35°C. Far-UV CD spectra were obtained at room temperature. The molar ellipticity was calculated from the observed ellipticity using following equation,

$$[\theta] = 100 \times (\theta / c \times l) \quad (1)$$

where c is the concentration of the protein in mol/dm^3 and l is the path length of the cuvette in centimeters. The baseline correction was done for each spectrum and was taken as an average of three accumulations (scan rate, 100 nm/min).

Anilino naphthalene sulfonate (ANS)-binding assay

An ANS-binding assay was performed to examine the effect of VinPhe-Nos on the structural integrity of tubulin. Tubulin (2 μM) was incubated with different concentrations of VinPhe-Nos (0–100 μM) for 30 min at 35°C in PEM buffer (50 mM Pipes, 1 mM EGTA, 3 mM $MgSO_4$, pH6.8). After the incubation, ANS (50 μM) was added and the samples were incubated for an additional 20 min. The samples were then excited at 380 nm and the emission spectra were recorded (400–500 nm). The experiment was repeated twice in duplicates.

Colchicine-binding assay

To gain insights into the nature of binding of VinPhe-Nos to tubulin, we investigated whether the compound binds at the colchicine site on tubulin, as follows: Tubulin (3 μM) was incubated with different concentrations of VinPhe-Nos (0–70 μM) at 35°C for 30 min. Subsequently, 10 μM colchicine was added, and the samples incubated for an additional 60 min at 35°C. The samples were then excited at 360 nm and the emission spectra were recorded (380–550 nm). The experiment was repeated twice.

Effect of VinPhe-Nos on microtubule assembly

Tubulin (12 μM) was polymerized in the absence or presence of VinPhe-Nos (0–200 μM) or 10 μM nocodazole in PEM buffer, in the presence of 1 M glutamate and 1 mM GTP, at 35°C for 45 min. The samples were then centrifuged in a Beckman Coulter Aventi J/26S XP centrifuge (Beckman Coulter, Brea, CA) using a JA-18.1 rotor at 35,000 ×g; 35°C; 45 min. After centrifugation, supernatants were aspirated off, and pellets dissolved in equal amount of water by incubating them at 4°C overnight. Next day, protein concentrations were measured using a Bradford assay. The experiment was repeated twice. In order to further examine the effect of VinPhe-Nos on microtubule assembly, a light scattering assay was performed. The reaction mixture, prepared as mentioned for the polymer mass assay, was transferred to a spectrofluorometer attached to a water-circulating bath set at 35°C. The polymerization was monitored through 90° light scattering after setting the excitation and emission wavelengths at 500 nm. Once the assembly reached steady state, VinPhe-Nos (50 μM) was added to the sample and the reading continued up to 50 min. The experiment was repeated twice.

Molecular modeling of VinPhe-Nos as a tubulin-binding agent

Homology model building of isotype-specific β-tubulin

To investigate the binding affinity of VinPhe-Nos with specific isotypes of β-tubulin in the αβ-heterodimer, we

constructed tubulin structures comprised of α-tubulin and different isotypes of β-tubulin. The protein sequences of eight human β-tubulin isotypes [β_I to β_{VIII}] were downloaded from the NCBI database. The representative sequences of β-isotypes, β_I (gi: 18088719), β_{II} (gi: 29788768), β_{III} (gi: 1297274), β_{IV} (gi: 135470), β_V (gi: 14201536), β_{VI} (gi: 62903515), β_{VII} (gi: 1857526), and β_{VIII} (gi: 42558279), were used to build the modeled structure of tubulin heterodimers based on homology modeling and by using the co-crystallized structure of the colchicine-tubulin complex (PDB ID: 1SA0, resolution 3.58 Å) as the templates (Santoshi & Naik, 2014). This representative structure of colchicine-tubulin complex was refined to adjust hydrogens, bond order, deleted water molecules, hydrogen bond network, and protonation at pH 7.0, using the protein preparation wizard. Furthermore, the structure was stabilized by performing 10 ns MD simulation, as described earlier (Santoshi & Naik, 2014) and used as template. All the modeled structures of tubulin isotypes were refined by performing an all-atom MD simulation of 10 ns, and validated using PROCHECK, ERRAT, and VERIFY3D, as reported earlier (Santoshi & Naik, 2014).

Molecular building and structure optimization of VinPhe-Nos

Molecular structure of VinPhe-Nos was built using Maestro (version 9.2, Schrödinger) and was energy minimized using Macromodel (version 9.9, Schrödinger) and OPLS 2005 force field with PRCG algorithm (1000 step minimization with an energy gradient of .001). Ligprep (version 2.5, Schrödinger) was used to assign appropriate bond order. The molecular structure was geometrically optimized using hybrid density functional theory with Becke's three-parameter exchange potential and the Lee-Yang-Parr correlation functional (B3LYP). Jaguar (version 7.7, Schrödinger, LLC) was used for the geometrical optimization of the ligand as reported (Mahaddalkar et al., 2015).

Molecular docking of VinPhe-Nos with tubulin isotypes and prediction of binding free energy

VinPhe-Nos was docked into the predicted noscapinoid binding site at the interface of different αβ-tubulin isotypes using "Extra Precision" (XP) algorithm of Glide docking (version 5.7, Schrödinger) (Santoshi & Naik, 2014). The binding site was fixed using a concentric grid box of size 12 Å × 12 Å × 12 Å at the centroid by means of the Glide grid-receptor generation program. A scale factor of .4 for van der Waals radii was applied to atoms of tubulin with absolute partial charges less than or equal to .25. The binding site amino acids within 8 Å of the docked ligand were extracted and analyzed for differences in molecular interactions with respect to each β isotypes. To stabilize the complex, the single best docked conformation of the VinPhe-Nos complexed with the tubulin isotype was used as the initial conformation for MD simulation of 10 ns. We have performed an all atom MD simulation of the complex in explicit water using AMBER 11.0 and the AMBER ff99SB force field for the tubulin and general AMBER (GAFF) force field for VinPhe-Nos on a time scale of 10 ns (Santoshi & Naik, 2014). The complex structure of VinPhe-Nos with the tubulin isotype was solvated with TIP3P water model (included in the AMBER package) by enclosing the complex in an octahedral three-dimensional periodic boundary condition with a distance of 15 Å between the wall of the box and the closest atom of the complex. To neutralize the system, 31 Na^+ counter ions were added. The molecular system was then energy minimized using 500 steps of steepest descent energy minimization, followed by 500 steps of conjugate gradient energy minimization, in three consecutive rounds with the force constants of 10 $kcal^{-1}$ $Å^{-2}$ and 2 $kcal^{-1}$ $Å^{-2}$, respectively. Positional restraints were applied to the whole system for the first and second round to relax the solvent molecules, whereas in the third round the whole system was minimized without any restraints. The electrostatic term was described using the Particle Mesh Ewald algorithm (Daren, York, & Pedersen, 1993). Finally, a 10 ns MD simulation was carried out following 200 ps of equilibration at 300 K, with a time step of 2 fs that generated a total of 5000 frames. The temperature of the system was regulated using the langevin thermostat. All equilibration and subsequent MD stages were carried out in an isothermal isobaric (NPT) ensemble using a Berendsen barometer with a target pressure of 1 bar, recording trajectories every 2 ps. A total of 1000 snapshots, generated from the last 2 ns of the MD trajectory for each molecular species, were considered to create the average structure for computation of binding free energy (ΔG_{bind}) of VinPhe-Nos using Prime molecular mechanics generalized Born solvation area (Prime/MM-GBSA). The docked poses of VinPhe-Nos was energy-minimized using the local optimization feature in Prime (Schrodinger package) and the energies of complex was calculated using the OPLS-AA force field and generalized-Born continuum solvent model. The binding free energy (ΔG_{bind}) was then estimated using the following equation,

$$\Delta G_{bind} = E_{R:L} - (E_R + E_L) + \Delta G_{solv} + \Delta G_{SA} \qquad (2)$$

where $E_{R:L}$ is energy of the VinPhe-Nos–tubulin complex, $E_R + E_L$ is the sum of the energies of the VinPhe-Nos and tubulin alone, using the OPLS-AA force field. ΔG_{solv} (ΔG_{SA}) is the difference between GBSA solvation energy (surface area energy) of complex and sum of the corresponding energies for the VinPhe-Nos and tubulin alone.

Results

VinPhe-Nos inhibited MDA-MB-231 cell proliferation

We investigated the ability of VinPhe-Nos (Figure 1(A)) to inhibit viability of an aggressive breast cancer cell line, MDA-MB-231, by exposing the cells to the drug for 72 h. The noscapinoid inhibited the cell proliferation in a concentration-dependent manner (Figure 1(B)). For example, 3, 6, and 25 µM VinPhe-Nos inhibited cell proliferation by 26, 50, and 80% respectively, yielding an average IC_{50} of 6 ± .6 µM (Figure 1(B)).

VinPhe-Nos binding induced changes in secondary structure of tubulin

To delineate the drug-induced conformational changes of secondary structure of tubulin by VinPhe-Nos, CD spectra of tubulin were acquired after incubating the protein with VinPhe-Nos. As illustrated in Figure 2(A), VinPhe-Nos altered the far-UV circular dichroism spectrum of the tubulin, indicating that the noscapinoid indeed bound tubulin and induced a loss of helical stability in the protein.

VinPhe-Nos altered the surface features of tubulin

Based on the *in vitro* finding that VinPhe-Nos binds to tubulin and altered its secondary structure (Figure 2(B)), we next tested the effect of this noscapinoid on tubulin's tertiary conformation using ANS, a fluorescent probe that binds hydrophobic patches on proteins. VinPhe-Nos-treated tubulin showed considerable, consistent, concentration-dependent increase in tubulin-ANS fluorescence (Figure 2(B)). For example, compared to the control, 70 and 100 µM VinPhe-Nos increased the fluorescence by 16 and 40% respectively, indicating that the compound altered the surface features of tubulin and exposed the hydrophobic residues in a concentration-dependent manner.

Promotion of colchicine binding to tubulin by VinPhe-Nos

After identifying that VinPhe-Nos binds tubulin and alters its secondary and tertiary configurations, we probed its putative binding site on the protein using a colchicine-binding assay. As shown in Figure 2(C),

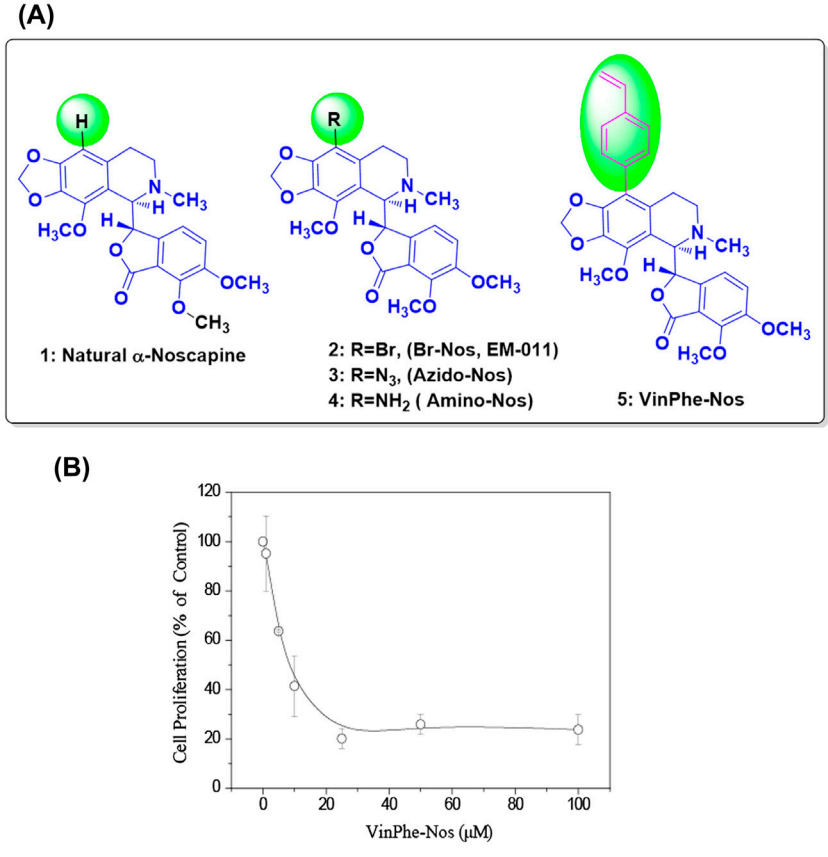

Figure 1. VinPhe-Nos, and its effects on MDA-MB-231 viability. (A) 9-(4-vinylphenyl) noscapine (VinPhe-Nos) was synthesized from noscapine. (B) Inhibition of MDA-MB-231 cell proliferation by VinPhe-Nos. Error bars, mean ± SD of three independent experiments.

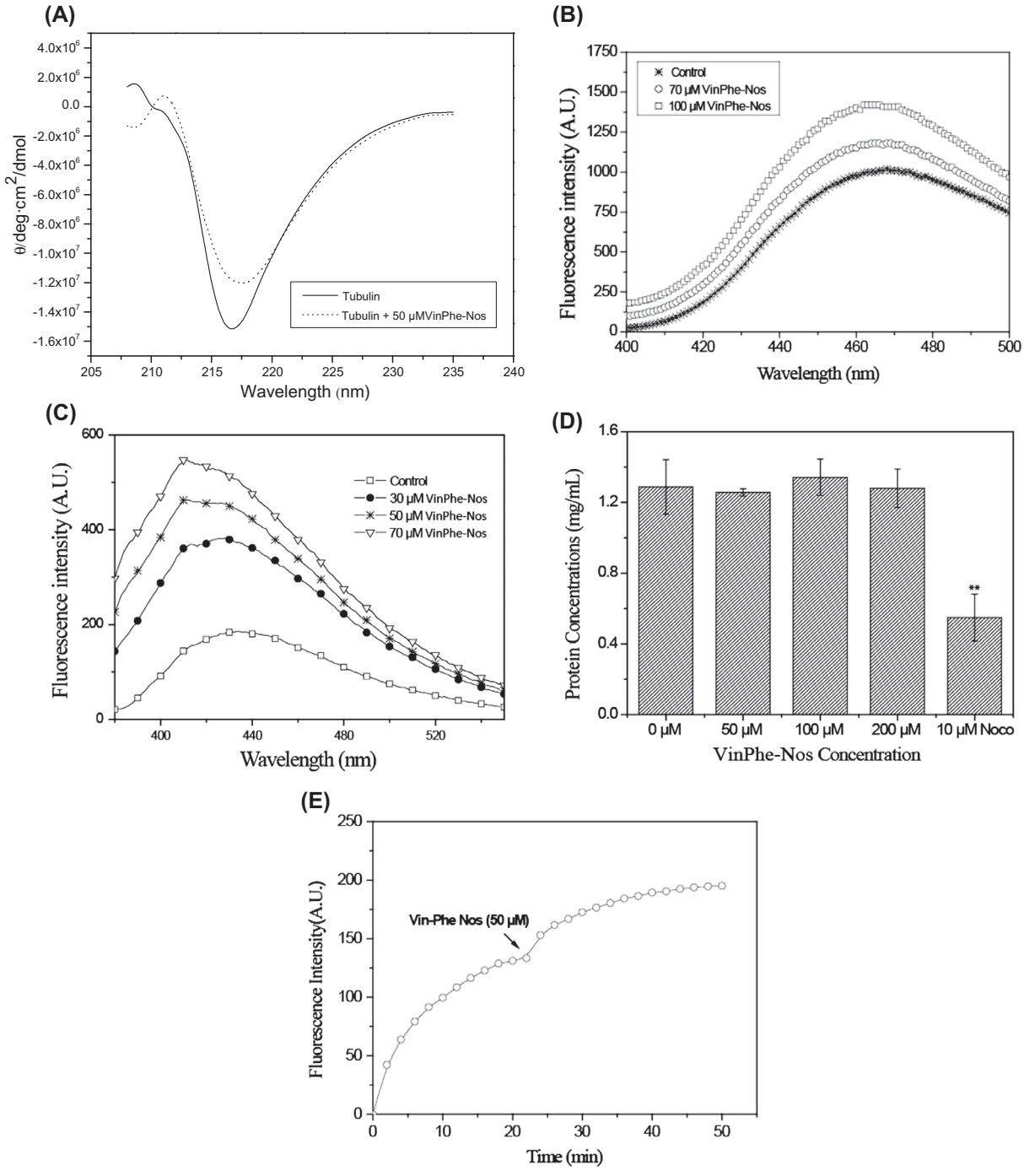

Figure 2. Characterization of VinPhe-Nos–tubulin interactions. (A) Far-UV circular dichroism spectra in the presence of VinPhe-Nos indicating loss of helical stability in tubulin in the presence of the drug. (B) VinPhe-Nos altered surface features of tubulin and increased ANS binding to tubulin in a concentration-dependent manner. (C) Promotion of colchicine binding to tubulin by VinPhe-Nos. For A–C, the graphs represent one of the three independent experiments. (D) VinPhe-Nos did not alter microtubule polymer mass. The experiment was repeated twice. (E) Lack of inhibition of microtubule assembly by VinPhe-Nos as monitored by a light-scattering assay. The graph is a representative of three independent experiments. $^{**}p < .01$, vs. control (Students' *t* test).

VinPhe-Nos did not inhibit colchicine binding to tubulin as evidenced by an apparent lack of reduction in the tubulin-colchicine fluorescence in the presence of the drug. Conversely, as illustrated in Figure 2(C), VinPhe-Nos enhanced the binding of colchicine to tubulin, suggesting that the drug did not completely masked

the colchicine binding site and that it could promote colchicine binding to tubulin.

VinPhe-Nos did not alter microtubule assembly considerably

When assembled in their presence, the majority of tubulin-binding agents either inhibits or promotes the polymer mass of tubulin (Lopus, Yenjerla, & Wilson, 2008). Therefore, we next asked whether VinPhe-Nos promotes or inhibits microtubule polymerization. As shown in Figure 2(D), VinPhe-Nos (0–200 μM) did not reduce the mass of assembled microtubules. Nocodazole – a drug known for its ability to inhibit microtubule polymer mass – did so in our assay condition as well. Specifically, 10 μM nocodazole reduced the polymer mass by 59% (Figure 2(D)), suggesting that synthetic alterations of VinPhe-Nos do not change the general mechanism of action of noscapine on microtubule assembly. In order to further examine the effect of VinPhe-Nos on microtubule assembly, a light scattering assay was performed wherein tubulin was assembled in the absence of the drug for 22 min to allow the assembly to reach steady state. Afterwards, VinPhe-Nos (50 μM) was added to the reaction mixture and the assembly continued until 50 min. As shown in Figure 2(E), the drug did not inhibit microtubule assembly. The turbidity scattering showed only a slight *increase* in assembly, indicating that, like the parent compound, VinPhe-Nos is not a strong inhibitor of microtubule assembly.

Table 1. Results of molecular docking (Glide XP) and prime MM-GBSA of VinPhe-Nos with different αβ-tubulin isotypes.

Tubulin isotype	Docking score (kcal/mol)	ΔG_{bind} (kcal/mol)
$\alpha\beta_{I}$	−6.835	−76.029
$\alpha\beta_{II}$	−5.751	−57.213
$\alpha\beta_{III}$	−7.905	−98.397
$\alpha\beta_{IV}$	−6.444	−73.883
$\alpha\beta_{V}$	−5.989	−62.785
$\alpha\beta_{VI}$	−4.561	−46.291
$\alpha\beta_{VII}$	−6.357	−73.229
$\alpha\beta_{VIII}$	−4.951	−56.897

Molecular characterization of the binding of VinPhe-Nos to specific isotypes of β-tubulin

After confirming that VinPhe-Nos binds tubulin, we determined its binding affinities with specific β-tubulin

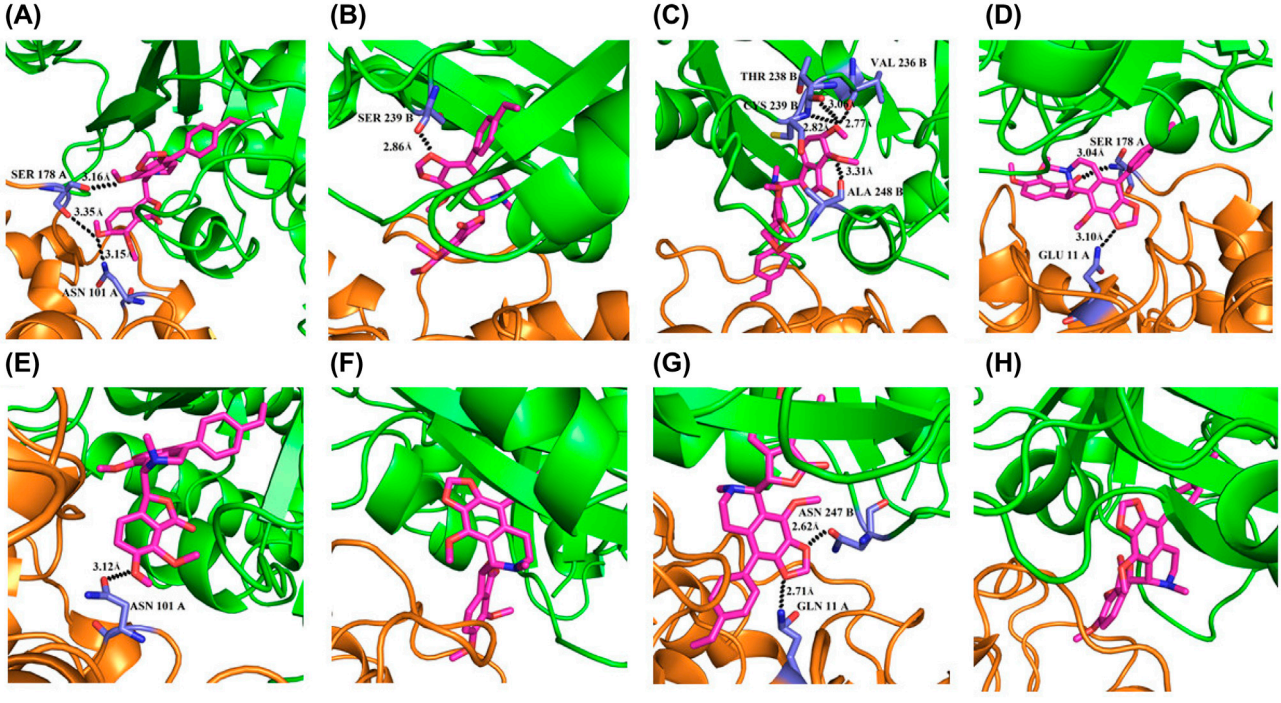

Figure 3. The binding mode of VinPhe-Nos with different β-tubulin isotypes showing difference in molecular interactions and hydrogen bonding pattern. The hydrogen bonding pattern revealed in the complexes of VinPhe-Nos with respect to (A) β_I isotype, showing three hydrogen bonds; (B) β_{II} isotype, showing one hydrogen bond; (C) β_{III} isotype, showing four hydrogen bonds (the fifth one is hidden in this image; see Figure 4); (D) β_{IV} isotype, showing two hydrogen bonds; (E) β_V isotype, showing one hydrogen bond; (F) β_{VI} isotype, showing no hydrogen bond; (G) β_{VII} isotype, showing two hydrogen bonds, and (H) β_{VIII} isotype, showing no hydrogen bond with the binding site amino acids.

isotypes in the αβ-heterodimer using molecular docking, MD simulation, and MM-GBSA calculations (Mahaddalkar et al., 2015; Naik, Santoshi, Rai, & Joshi, 2011). The Glide docking program validates different positions, orientations, and conformations of the ligands inside the binding site in a systematic manner, and returns the best docked configuration of the ligand. We performed exhaustive sampling using the parameters presented in Glide extra precision (XP) method. The reproducibility of the docking method was validated by redocking the extracted colchicine from its cognate structure (1SA0) and by comparing with the crystal structure (the top 6 poses of Glide XP docking showed root-mean-square deviation (RMSD) in between .19 and 1.06 Å with the crystal structure). Glide-XP docked VinPhe-Nos at the noscapinoid binding site on tubulin as reported earlier (Naik et al., 2011) and calculated the binding affinity (glide score). As shown in Table 1, the glide score of VinPhe-Nos was found to be substantially different for different β-tubulin isotypes. Specifically, the noscapinoid showed the lowest glide score of −7.905 kcal/mol with $\alpha\beta_{III}$ tubulin, followed by −6.835, −6.444, −6.357, −5.989, −5.751, −4.951, and −4.561 kcal/mol with $\alpha\beta_{I}$, $\alpha\beta_{IV}$, $\alpha\beta_{VII}$, $\alpha\beta_{V}$, $\alpha\beta_{II}$, $\alpha\beta_{VIII}$, and $\alpha\beta_{VI}$, respectively, indicating highest predictive binding affinity of VinPhe-Nos toward β_{III} tubulin isotype. A possible reason for the variations in the glide score with different β-tubulin isotypes could be the variations in binding mode due to differences in binding-site amino acids. In order to stabilize the docked complex of

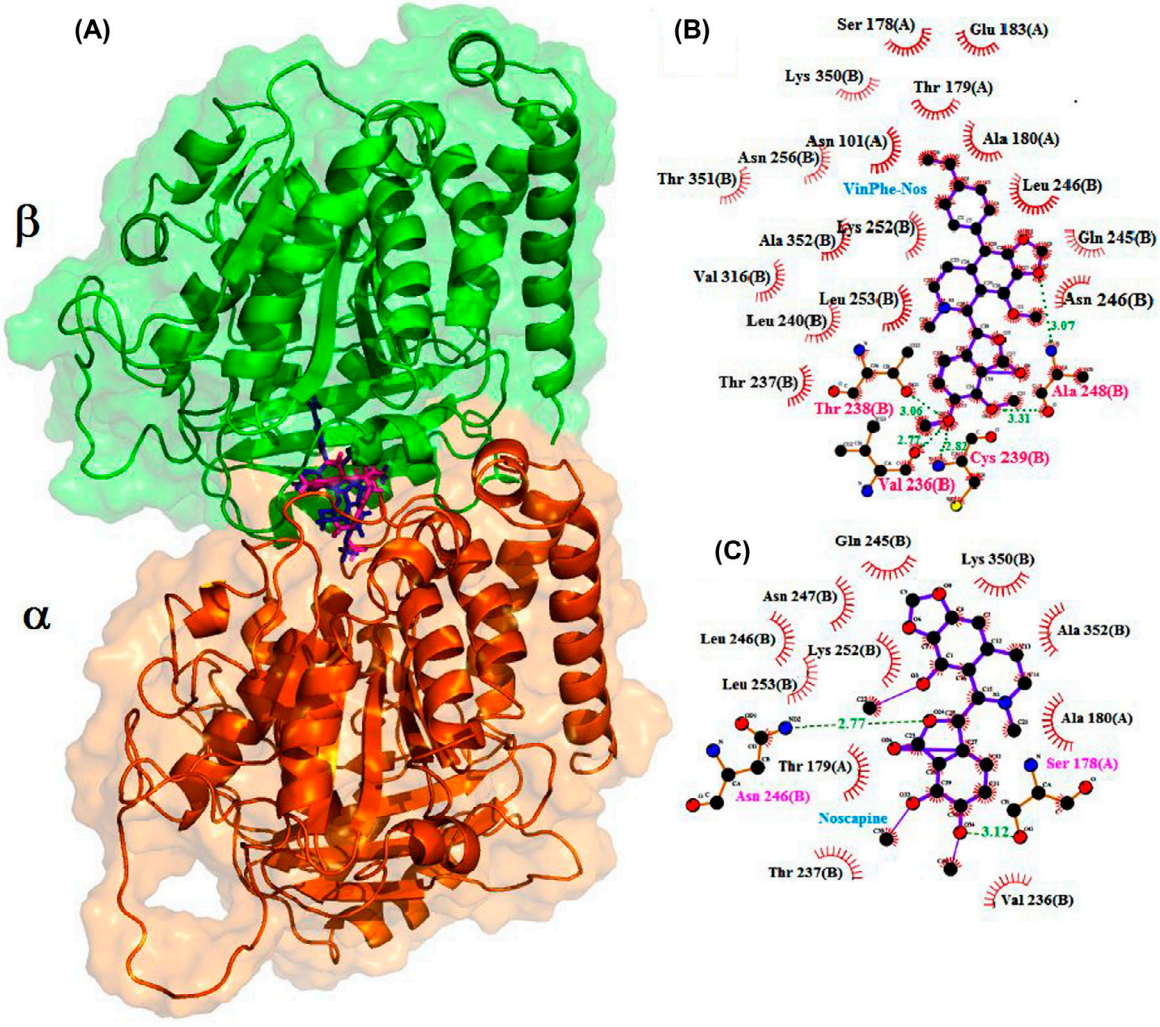

Figure 4. Comparison of binding modes of VinPhe-Nos with β_{III} tubulin, and noscapine with β_{III} tubulin. Panel (A) shows the docked poses of VinPhe-Nos (blue) and noscapine (red) bound to β_{III} tubulin at noscapine-binding site. Panel (B) and (C) shows the ligplot of binding site amino acids involved in hydrogen bonding and hydrophobic interactions with VinPhe-Nos and noscapine, respectively. There are five hydrogen bonds involved in the binding of VinPhe-Nos with the β_{III} tubulin whereas noscapine- β_{III} tubulin interaction involved only two hydrogen bonds.

VinPhe-Nos and each αβ-tubulin isotype, and to elucidate the molecular interaction(s), we performed the MD simulation of 10 ns, taking the best docked complex from each molecular species. The stability of the system was monitored by RMSD of Cα-atoms during the entire duration of the simulation as shown in Supplementary Figure 1. VinPhe-Nos observed to dock onto different β-tubulin isotypes throughout the 10 ns simulation. The average structure of docked complexes was generated out of the 1000 frames obtained every 2 ps from the last 2 ns of MD trajectory, and was used to elucidate the binding mode of the compound to the tubulin isotypes. Analysis of the binding mode of VinPhe-Nos revealed variations in hydrogen bonding patterns. Specifically, β_I, β_{II}, β_{III}, β_{IV}, β_V, β_{VI}, β_{VII}, β_{VIII}, showed 3, 1, 5, 2, 1, 0, 2, and 0 hydrogen bonds, respectively (Figure 3), indicating that the highest-affinity binding of VinPhe-Nos to β_{III} was due to the involvement of 5 hydrogen bonds. Ala 248, although it provided two hydrogen bonds, does not show both of them on the 3D image (Figure 3) because of the orientation of one of the bonds. However, the ligprep sketch showed the hidden hydrogen bonds (Figure 4). Cys 239, Val 236, Thr 238 provided one hydrogen bond each to strengthen the binding of VinPhe-Nos to β_{III} tubulin (Figure 4). The data also suggests that, although all the hydrogen bonds were provided by the amino acids of β tubulin, VinPhe-Nos–tubulin interaction involves interactions with both α- and β-tubulin; the binding was biased toward β-tubulin across all αβ-tubulin isotypes. However, the contribution of hydrophobic interactions in the binding of VinPhe-Nos with tubulin cannot be ruled out because the binding pocket consists of several non-polar amino acids. The molecular interaction of VinPhe-Nos with tubulin is attributed to the formation of both hydrogen bonds and hydrophobic interactions with the surrounding amino acids (Figure 4). Interestingly, noscapine binding to β_{III}-tubulin involved only two H bonds (Figure 4), indicating the superior affinity of VinPhe-Nos to β_{III}-tubulin, compared to the parent compound. Both the VinPhe-Nos and noscapine were well accommodated inside the binding cavity (Figure 4). Moreover, the predictive binding free energy (ΔG_{bind}) based on Prime MM-GBSA with different αβ-tubulin isotypes (Table 1) indicated that VinPhe-Nos binds more tightly to the β_{III}-tubulin isotype (−98.397 kcal/mol) compared to other isotypes. The differential molecular interactions and binding free energy of VinPhe-Nos with different αβ-tubulin isotypes suggest that the noscapinoid has different specificities to different β-tubulin isotypes and that it has highest affinity to the β_{III}-tubulin isotype.

Discussion

In this study, we investigated the binding interactions of VinPhe-Nos, an analog of the opium-derived natural product, noscapine (Santoshi et al., 2015), with its cellular target, tubulin. This biaryl pharmacophore-inserted noscapine was designed in light of the previous reports on antiproliferative efficacy of biaryl group-containing agents that target tubulin (Santoshi et al., 2015). After observing that VinPhe-Nos is six times more potent than the parent compound in inhibiting survival of an aggressive breast cancer cell line, MDA-MB-231 (Figure 1(B)), we investigated its general mode of binding to tubulin based on the methodologies of circular dichroism, spectrofluorimetric, turbidimetric, and sedimentation techniques. After elucidating its general binding interactions with tubulin and its effect on tubulin assembly, we performed computational docking and MD simulations to decipher its modes of binding to all known isotypes of β tubulin to examine its relative affinity to each isotype.

VinPhe-Nos showed superior efficacy in inhibiting MDA-MB-231 cell proliferation as compared to noscapine

As reported earlier (Santoshi et al., 2015), VinPhe-Nos (Figure 1(A)) inhibits proliferation of several human cancer cell lines, including cervical carcinoma (HeLa) (IC_{50}, 20 μM), lung carcinoma (A549) (IC_{50}, 43 μM), and breast carcinoma (MCF-7) (IC_{50}, 34 μM). For the current study, we used an *in vitro* cell viability assay to determine the concentration of VinPhe-Nos required to inhibit MDA-MB-231 cell survival by 50%, after exposing the cells to the drug for 72 h. The IC_{50} of VinPhe-Nos for MDA-MB-231 cells was found to be considerably lower (6 ± .6 μM; Figure 1(B)). Compared to the parent compound noscapine, which inhibits MDA-MB-231 cell proliferation with an IC_{50} of 36 ± 4 μM (Chougule, Patel, Jackson, & Singh, 2011), our finding suggest that VinPhe-Nos is approximately six times more potent than noscapine.

Biochemical characterization of VinPhe-Nos–tubulin interactions

We started our molecular-level characterization of the binding interactions between VinPhe-Nos and tubulin by examining its effect on the secondary structure of tubulin using circular dichroism measurements at far-UV range, and found that VinPhe-Nos induces changes in tubulin secondary structure (Figure 2(A)). We further found, using an ANS binding assay, that the binding of VinPhe-Nos to tubulin altered the tertiary conformation of the protein as well (Figure 2(B)). ANS, at its non-protein-bound state, shows negligible fluorescence emission when excited at 380 nm, but the fluorescence enhances multiple folds when it is bound to hydrophobic patches on proteins (Mahaddalkar et al., 2015). The concentration-dependent increase of ANS fluorescence of

VinPhe-Nos-treated tubulin suggests that the compound exposed hydrophobic patches of tubulin. VinPhe-Nos enhanced colchicine binding to tubulin (Figure 2(C)). Colchicine binds tubulin at the intra-dimer interface assisted by its tropolone moiety and the A-ring. The tropolone moiety at its protein-bound state fluoresces when excited at the specified wavelength (Bhattacharyya & Wolff, 1974). Our data (Figure 2(C)) suggests that VinPhe-Nos, while itself not binding to the colchicine site (as evidenced by an apparent lack of reduction of tubulin-colchicine fluorescence in the presence of the drug), promoted colchicine binding (Figure 2(C)). This finding corroborates with our earlier observation that noscapine and its derivatives bind at a site overlapping with colchicine binding site or a site very close to it (Naik et al., 2011) and thus might promote colchicine binding. The best way to understand the noscapinoid binding site is to obtain a co-crystal structure with tubulin, which is not yet possible due to instability of the tubulin structure. However, there must be some differences in the molecular interactions of noscapinoids that account for their net differences in the microtubule assembly reaction than colchicine. Importantly, from a clinical point of view, colchicine-site binding agents are known to overcome β_{III} tubulin-mediated drug resistance (Stengel et al., 2010). For example, the anticancer efficacy of the colchicine-site-binding agent 2-methoxyoestradiol and its derivatives, STX140 and STX243, was found to be unaltered by the changes in β_{III}-tubulin expression (Stengel et al., 2010). Here, we provide evidence that, in addition to drugs that bind directly to the colchicine site, those that enhance colchicine binding also hold potential as effective antitumour agents.

Noscapine does not alter microtubule polymer mass considerably (Lopus & Naik, 2015). Because we found VinPhe-Nos six times more potent than noscapine in inhibiting the cancer cell proliferation, we asked whether the chemical modifications have altered the compound's effect on the polymer mass of microtubules. We therefore examined the effect VinPhe-Nos on the assembly of tubulin subunits into microtubules *in vitro* using a sedimentation assay. VinPhe-Nos did not considerably alter the polymer mass (Figure 2(D)) or reduce extent of the tubulin assembly (Figure 2(E)), indicating that the structural alterations incorporated into noscapine for creating VinPhe-Nos (Figure 1(A)) did not change the general mode of action of noscapine on tubulin assembly. However, as mentioned earlier, the alterations substantially enhanced its antiproliferative potential (Figure 1(B)). Tubulin-binding compounds that do not show considerable effect on microtubule polymer mass are considered potential candidates for adjuvant therapy against cancer. For example, griseofulvin, isolated from *Penicillium griseofulvum*, does not alter microtubule polymer mass (Wehland, Herzog, & Weber, 1977), yet it synergistically inhibits MCF-7 cell proliferation with vinblastine (Rathinasamy et al., 2010), and is effective against multiple myeloma (Kim et al., 2011).

The molecular mechanism of action of VinPhe-Nos involves preferential binding to the β_{III} tubulin isotype

Overexpression of β_{III} tubulin has been associated with resistance against a wide spectrum of cancer drugs (Tseng et al., 2010). Therefore, it may be considered a molecular target for pharmacological intervention. For example, seco-taxoid, IDN 5390 (Pepe et al., 2009) was designed to bind explicitly to the taxane-binding site on β_{III} tubulin. Consequently, this drug has been found to be effective against paclitaxel-resistant cell lines that overexpress β_{III} (Pepe et al., 2009). We investigated the preferred binding mode and affinity of VinPhe-Nos to all well-characterized isotypes of β tubulin using molecular docking and MD simulations. The lowest predictive binding energy (−98.397 kcal/mol) and docking score (−7.905 kcal/mol) of VinPhe-Nos with β_{III} tubulin compared to other isotypes suggest that it binds with highest affinity to β_{III} tubulin (Figures 3 and 4). We have also compared the binding of the parent compound noscapine to β_{III} tubulin with VinPhe-Nos- β_{III} tubulin binding (Figure 4). Unlike noscapine, whose binding interaction with β_{III} tubulin involved only two hydrogen bonds, VinPhe-Nos binding showed involvement of five hydrogen bonds (Figure 4), demonstrating the superior binding efficacy of VinPhe-Nos to β_{III} tubulin over the parent compound. Our findings suggest the potential clinical utility of VinPhe-Nos against β_{III} tubulin-overexpressing tumors.

Supplementary material

The supplementary material for this article is available online at http://dx.doi.org/10.1080/07391102.2016.1222969.

Acknowledgment

The authors thank UM-DAE CBS (T.M, S.C., M.L) and DBT-Indo-Australia Biotechnology Fund (S.K.) for financial support.

Disclosure statement

No potential conflict of interest was reported by the authors.

References

Bhattacharyya, B., & Wolff, J. (1974). Promotion of fluorescence upon binding of colchicine to tubulin. *Proceedings of the National Academy of Sciences of the United States of America, 71*, 2627–2631.

Chougule, M. B., Patel, A. R., Jackson, T., & Singh, M. (2011). Antitumor activity of noscapine in combination with Doxorubicin in triple negative breast cancer. *PLoS One, 6*, e17733. doi:10.1371/journal.pone.0017733

Daren, T., York, D., & Pedersen, L. (1993). Particle mesh Ewald: An N-log(N) method for Ewald sums in large systems. *The Journal of chemical physics, 98*, 10089–10092. doi:10.1063/1.464397

Janke, C. (2014). The tubulin code: Molecular components, readout mechanisms, and functions. *The Journal of Cell Biology, 206*, 461–472. doi:10.1083/jcb.201406055

Kim, Y., Alpmann, P., Blaum-Feder, S., Krämer, S., Endo, T., Lu, D., … Schmidt-Wolf, I. G. (2011). *In vivo* efficacy of griseofulvin against multiple myeloma. *Leukemia Research, 35*, 1070–1073. doi:10.1016/j.leukres.2010.10.008

Lopus, M., & Naik, P. K. (2015). Taking aim at a dynamic target: Noscapinoids as microtubule-targeted cancer therapeutics. *Pharmacological Reports, 67*, 56–62. doi:10.1016/j.pharep.2014.09.003

Lopus, M., Smiyun, G., Miller, H., Oroudjev, E., Wilson, L., & Jordan, M. A. (2015). Mechanism of action of ixabepilone and its interactions with the βIII-tubulin isotype. *Cancer Chemotherapy and Pharmacology, 76*, 1013–1024. doi:10.1007/s00280-015-2863-z

Lopus, M., Yenjerla, M., & Wilson, L. (2008). Microtubule dynamics. *Wiley Encyclopedia in Chemical Biology, 3*, 153–160. doi:10.1002/9780470048672.wecb338

Mahaddalkar, T., Suri, C., Naik, P. K., & Lopus, M. (2015). Biochemical characterization and molecular dynamic simulation of β-sitosterol as a tubulin-binding anticancer agent. *European Journal of Pharmacology, 760*, 154–162. doi:10.1016/j.ejphar.2015.04.014

Naik, P. K., Santoshi, S., Rai, A., & Joshi, H. C. (2011). Molecular modelling and competition binding study of Br-noscapine and colchicine provide insight into noscapinoid-tubulin binding site. *Journal of Molecular Graphics and Modelling, 29*, 947–955. doi:10.1016/j.jmgm. 2011.03.004

Pepe, A., Sun, L., Zanardi, I., Wu, X., Ferlini, C., Fontana, G., … Ojima, I. (2009). Novel C-seco-taxoids possessing high potency against paclitaxel-resistant cancer cell lines overexpressing class III β-tubulin. *Bioorganic & Medicinal Chemistry Letters, 19*, 3300–3304. doi:10.1016/j.bmcl.2009.04.070

Rathinasamy, K., Jindal, B., Asthana, J., Singh, P., Balaji, P. V., & Panda, D. (2010). Griseofulvin stabilizes microtubule dynamics, activates p53 and inhibits the proliferation of MCF-7 cells synergistically with vinblastine. *BMC Cancer, 10*, 213–225. doi:10.1186/1471-2407-10-213

Santoshi, S., Manchukonda, N. K., Suri, C., Sharma, M., Sridhar, B., Joseph, S., … Naik, P. K. (2015). Rational design of biaryl pharmacophore inserted noscapine derivatives as potent tubulin binding anticancer agents. *Journal of Computer-Aided Molecular Design, 29*, 249–270. doi:10.1007/s10822-014-9820-5

Santoshi, S., & Naik, P. K. (2014). Molecular insight of isotypes specific heterodimer with noscapinoids. *Journal of Computer-Aided Molecular Design, 28*, 751–763. doi:10.1007/s10822-014-9756-9

Stengel, C., Newman, S. P., Leese, M. P., Potter, B. V., Reed, M. J., & Purohit, A. (2010). Class III β-tubulin expression and *in vitro* resistance to microtubule targeting agents. *British Journal of Cancer, 102*, 316–324. doi:10.1038/sj.bjc.6605489

Tseng, C. Y., Mane, J. Y., Winter, P., Johnson, L., Huzil, T., Izbicka, E., … Tuszynski, J. A. (2010). Quantitative analysis of the effect of tubulin isotype expression on sensitivity of cancer cell lines to a set of novel colchicine derivatives. *Molecular Cancer, 9*, 131. doi:10.1186/1476-4598-9-131

Wehland, J., Herzog, W., & Weber, K. (1977). Interaction of griseofulvin with microtubules, microtubule protein and tubulin. *Journal of Molecular Biology, 111*, 329–342. doi:10.1016/S0022-2836(77)80055-7